In situ modeling of acquired resistance to RTK/RAS pathway targeted therapies

Nancy E. Sealover*, Patricia L. Theard*, Amanda J. Linke, Jacob M. Hughes, Brianna R. Daley, and Robert L. Kortum

* These authors contributed equally to this paper

[1]Department of Pharmacology and Molecular Therapeutics, Uniformed Services University of the Health Sciences, Bethesda, MD

Corresponding Author: robert.kortum@usuhs.edu

Abstract

Intrinsic and acquired resistance limit the window of effectiveness for oncogene-targeted cancer therapies. Preclinical studies that identify synergistic combinations enhance therapeutic efficacy to target intrinsic resistance, however, methods to study acquired resistance in cell culture are lacking. Here, we describe a novel *in situ* resistance assay (ISRA), performed in a 96-well culture format, that models acquired resistance to RTK/RAS pathway targeted therapies. Using osimertinib resistance in *EGFR*-mutated lung adenocarcinoma (LUAD) as a model system, we show acquired resistance can be reliably modeled across cell lines using objectively defined osimertinib doses. Similar to patient populations, isolated osimertinib-resistant populations showed resistance via enhanced activation of multiple parallel RTKs so that individual RTK inhibitors did not re-sensitize cells to osimertinib. In contrast, inhibition of proximal RTK signaling using the SHP2 inhibitor RMC-4550 both re-sensitized resistant populations to osimertinib and prevented the development of osimertinib resistance as a primary therapy. Similar, objectively defined drug doses were used to model resistance to additional RTK/RAS pathway targeted therapies including the $KRAS^{G12C}$ inhibitors adagrasib and sotorasib, the MEK inhibitor trametinib, and the farnesyl transferase inhibitor tipifarnib. These studies highlight the tractability of in situ resistance assays to model acquired resistance to targeted therapies and provide a framework for assessing the extent to which synergistic drug combinations can target acquired drug resistance.

Introduction

Lung cancer is the leading cause of cancer-related death worldwide; adenocarcinomas are the most common subtype of lung cancer (*1*). Oncogenic driver mutations in the RTK/RAS/RAF pathway occur in 75-90% of lung adenocarcinomas (LUAD). With enhanced understanding of the oncogenic driver mutations causing disease, oncogene-targeted therapies have substantially improved patient outcomes not only for patients with LUAD, but across the spectrum of cancer types. However, in most cases resistance to targeted therapeutics develops necessitating novel approaches that can either delay therapeutic resistance or treat resistant cancers.

Historically, combination therapies have been based on identifying two or more active single agents with distinct mechanisms of action (*2*), and most current combination therapies include an oncogene-targeted therapy and a second drug that targets an independent mechanism that, if left targeted, causes resistance to the first agent (*3, 4*). While many of these approaches succeed in increasing windows of progression free survival (PFS) in patients, resistance still emerges, often due to the strikingly heterogeneous mechanisms of acquired drug resistance both intratumorally (*5, 6*) and across patients (*7, 8*). Thus, novel approaches are needed to identify combination therapies that not only address a single mechanism of acquired resistance but simultaneously prevent most common mechanisms of resistance to a given targeted therapy. This need has led to a shift toward groups attempting to identify synergistic drug combinations to treat cancers with specific genetic profiles (*2*).

Preclinical studies designed to identify synergistic drug combinations are excellent at capturing the success of a drug treatment within a timeframe of 1-14 days.

Unfortunately, few studies extend beyond assessing this initial window of efficacy to determine whether combinations can prevent the development of acquired resistance. For example, RNAi and CRISPR screens have been widely successful in identifying novel and often unexpected partners for combination therapies (*9-11*), however, the timeframe of these approaches biases them toward identifying and assessing secondary drug targets that will limit intrinsic, but not acquired, resistance. Further, those studies that do assess acquired resistance *in situ* are limited to the assessment of cell lines established by dose-escalation over multiple months (reviewed in (*12*)) (e.g. (*13-17*)) rather than determining the extent to which inhibiting a secondary drug target can delay the onset of resistance. While work using *in vivo* murine studies can assess a longer timeline of treatment efficacy (*18, 19*), the financial burden of these studies can limit their use when assessing multiple potential combination therapies. Therefore, a framework of pre-clinical experiments to assess initial efficacy combined with extended *in vitro* approaches such as 6-16 week proliferation outgrowth assays (*20, 21*) and time-to-progression (TTP) assays (*11*) can provide robust evidence for proposing effective and rational combination therapies that is accessible and scalable.

Here, we describe a novel *in situ* resistance assay (ISRA) that allows us to (i) assess the development of acquired resistance in a large cohort of individual cultures, (ii) isolate multiple therapy-resistant subclones for biochemical analysis, and (iii) test the effectiveness of combination therapies to delay the development of acquired resistance. We used *EGFR*-mutated LUAD cell lines as a model to assess the timeframe of acquired resistance to the third generation tyrosine kinase inhibitor (TKI) osimertinib in an *in situ* resistance assay (ISRA) that combines elements from proliferation outgrowth

(*21*) and TTP (*11*) assays, and allows for screening of drug combination in large numbers of individual cell populations using a 96-well format. Cells isolated from osimertinib ISRAs remain osimertinib resistant and can be used to identify effective drug combination therapies. Using a panel of inhibitors targeting multiple receptor tyrosine kinases (RTKs) and RTK-associated proteins, we found that inhibiting proximal RTK signaling using the SHP2 inhibitor RMC-4550 (*22*) most consistently increased both efficacy and potency of osimertinib across all osimertinib resistant cell lines. In addition to re-sensitizing osimertinib resistant lines to osimertinib, SHP2 inhibition both delayed the onset and reduced the overall frequency of osimertinib resistant cultures. This *in situ* resistance assay was broadly applicable to RTK/RAS pathway targeted therapies including $KRAS^{G12C}$ inhibitors sotorasib and adagrasib, the MEK inhibitor trametinib, and the FTI tipifarnib.

Results

Development of an assay to model acquired resistance *in situ*

We sought to develop an *in situ* resistance assay (ISRA) that modeled the development of acquired resistance to targeted therapies and could be performed in a multi-well setup to mimic a multiple-subject trial testing the effectiveness of drug combinations to limit the development of resistance. To develop and optimize the ISRA, we used a panel of *EGFR*-mutated lung adenocarcinoma (LUAD) lines treated with the third-generation TKI osimertinib, as the mechanisms driving osimertinib resistance in LUAD are well established (*23-32*). To establish the doses of osimertinib that inhibits survival (≥ EC_{50}) in the panel of *EGFR*-mutated cell lines, H1975, H827, PC9, and PC9-TM cells were treated with increasing doses of osimertinib and cell viability was assesses four days after treatment (Fig. 1A and B). The doses of osimertinib that inhibited survival were similar across all *EGFR*-mutated cell lines [EC_{50} (17-46 nM) - EC_{85} (200-450 nM)], allowing us to use similar doses in each cell line to determine the concentration of osimertinib that caused prolonged growth arrest (> 6 weeks) prior to cell outgrowth in a majority of cell populations for each cell line. Cells were plated at low density in multiple 96-well plates and each plate was either left untreated (to assess the time required for normal cell outgrowth) treated with a single inhibitory dose of osimertinib (EC_{50}-EC_{85} range; 30, 50, 150, or 300 nM) for up to 12 weeks. The inner 60 wells of each plate were visually assessed weekly and wells that were ≥ 50% confluent were scored as resistant to that dose of osimertinib. Lower doses of osimertinib corresponding to the EC_{50}-EC_{75} caused a 1–3-week delay in the outgrowth of cells, whereas cells treated with ≥ EC_{80} of osimertinib showed prolonged growth arrest before

regaining proliferative capacity (Fig. 1C), indicating that these wells had become osimertinib resistant.

We expanded a cohort of osimertinib-resistant populations (OR1-7) from H1975 cells treated with 150-300 nM osimertinib to investigate the extent to which (i) individual populations maintained osimertinib resistance and (ii) the mechanisms driving osimertinib resistance in cells isolated from continued drug treatment were similar to those seen in patient populations. Dose-response studies showed that osimertinib was much less potent in all seven OR populations compared to H1975 parental cells (Fig. 1D and fig. S1A), with >40% of cells surviving when treated with 1M osimertinib compared to < 20% of parental controls. Further, in ISRAs performed using 150 nM osimertinib, all seven populations showed osimertinib resistance (Fig. 1E and S1B). Parental H9175 cells showed a median PFS of ~9-weeks, with 70% of wells becoming resistant in the 12-week assay. In contrast OR1-7 populations showed outgrowth in 100% of wells within 3-5 weeks (Fig. 1E). These data confirm that cell populations isolated from ISRAs maintain drug resistance.

RTK phosphorylation is heterogeneously upregulated in osimertinib-resistant cells

Osimertinib resistance occurs by both EGFR-dependent and EGFR-independent mechanisms, however, unlike with 1st-generation EGFR-TKIs, EGFR-independent mechanisms predominate (*23, 25-27*). To test for EGFR-dependent osimertinib resistance in isolated OR populations, we sequenced the kinase domains of 25 OR populations, however, no mutations were found (data not shown). The most common

EGFR-independent mechanisms involve reactivation of RTK/RAS signaling caused by either mutation or increased expression of parallel RKTs (*23-32*) including MET (*24*), FGFR (*33, 34*), IGF1R (*28, 35*), RET (*36*), and AXL (*29-31*), among others (*7*); and simultaneous activation of multiple RTKs often occurs within the same patient (*5*). We evaluated OR cell lines for changes in magnitude of receptor tyrosine phosphorylation compared to parental H1975 cells using phospho-tyrosine RTK arrays (Fig. 2A and S3). OR1-7 cells showed increased phosphorylation of multiple RTKs; AXL and FGFR2-α were most consistently phosphorylated across OR1-7 populations with additional RTKs including c-MET, RET, IGF1R, c-KIT, TIE2, and EPH receptors and non-receptor kinases ABL and the SRC family kinases (SFKs) showing increased phosphorylation in at least two OR populations (Fig. 2A and S3). These data show that osimertinib-resistant populations isolated from ISRAs model the types of resistance seen in patient populations.

The current treatment paradigm for treating patients with osimertinib-resistant cancers is to determine therapy based on the mechanism(s) driving osimertinib resistance. We therefore examined the extent to which inhibitors (Fig. 2B) of RTKs or non-receptor tyrosine kinases activated in OR1-7 cells (Fig. 2A) synergized with osimertinib in OR1-7 cells. Since OR1-7 populations all showed activation of multiple RTKs, we further assessed osimertinib in combination with the SHP2 inhibitor RMC-4550 as a general inhibitor of proximal RTK signaling. Cells were treated either with increasing doses of osimertinib +/- 100 or 300 nM of the second inhibitor or increasing doses of the second inhibitor +/- 10 nM osimertinib (Fig. S4). Synergistic drug-drug interactions were assessed by Multi-dimensional Synergy of Combinations (MuSyC) to

deconvolute synergistic efficacy [Log(α_1) and Log(α_2)] and potency (β) (*37, 38*). Overall, the effects of specific RTK inhibitors or dasatinib was heterogenous among OR cell lines (Fig. 2C). In contrast, the SHP2 inhibitor RMC-4550 increased the efficacy [Log(α_2)] and potency (β_{obs}) of osimertinib in all osimertinib resistant populations (Fig. 2C). To further characterize the extent to which RMC-4550 synergized with osimertinib in osimertinib-resistant populations, we treated parental H1975 or OR1-7 with increasing doses of RMC-4550 and/or osimertinib in a 6x10 matrix of drug combinations and assessed for synergistic killing after 96 hours both by Bliss Independence (Fig. 2D) and MuSyC (Fig. 2E). Here again, SHP2 inhibition markedly enhanced the killing effects of osimertinib in OR1-7 cells, showing an increased excess over Bliss across the matrix of drug combinations (Fig. 2D) that was due to RMC-4550 enhancing both the efficacy [Log(α_2)] and potency (β_{obs}) of osimertinib (Fig. 2E). These data suggest that inhibiting proximal RTK signaling has the potential to overcome RTK-driven osimertinib resistance in *EGFR*-mutated cancers.

SHP2 inhibition synergizes with osimertinib treatment to limit the development of osimertinib resistance

Rapid autopsy studies assessing resistance to first- or second-line osimertinib showed that patients develop tumors harboring multiple parallel resistance mechanisms so that treatment of resistant tumors may be impractical (*5*). Thus, developing therapeutic approaches that delay the onset of osimertinib resistance has the potential to have a much greater impact on patient survival than treating resistance once it emerges. To directly assess the extent to which SHP2 inhibition could limit the

development of acquired osimertinib resistance, we performed ISRAs in *EGFR*-mutated H1975 and PC9 cells treated with osimertinib either alone in combination with two distinct SHP2 inhibitors [RMC-4550 or SHP099 (Fig. 3)]. When treated with osimertinib alone at either 150 or 300 nM, H1975 cells show a median survival of 9 weeks with 63% of populations eventually becoming osimertinib resistant. Combining RMC-4550 [HR: 0.05, 95% CI 0.03-0.07] or SHP099 [HR: 0.24, 95% CI 0.17-0.37] with osimertinib significantly inhibited the development of osimertinib resistance, with only 3% (RMC-4550) or 21% (SHP099) of populations treated with combination therapy showing outgrowth at 12-weeks.

Similar results were observed in PC9 cells treated with 300 nM osimertinib, where cells treated with osimertinib alone showed at median survival of 8 weeks and 76% of total populations became osimertinib resistant. Combining RMC-4550 [HR: 0.25, 95% CI 0.19-0.34] or SHP099 [HR: 0.44, 95% CI 0.34-0.57] with 300 nM osimertinib significantly inhibited the development of osimertinib resistance, with only 30% (RMC-4550) or 41% (SHP099) of populations treated with combination therapy showing outgrowth at 12-weeks. Further, while PC9 cells treated with 150 nM osimertinib show rapid outgrowth (median PFS 4 weeks), this outgrowth was significantly delayed by either RMC-4550 [HR: 0.28, 95% CI 0.21-0.36] or SHP099 [HR: 0.31, 95% CI 0.24-0.39]. Overall, these data show both the utility of ISRAs to test whether therapeutic combinations can inhibit the development acquired resistance and that proximal RTK inhibition has the potential to enhance the therapeutic window for patients with *EGFR*-mutated cancers on osimertinib.

Modeling resistance to KRAS^{G12C} inhibitors, trametinib, and tipifarnib

Oncogenic driver mutations in the RTK/RAS/RAF pathway occur in 75-90% of LUAD and, similar to *EGFR*-mutated LUADs treated with osimertinib, acquired resistance to targeted therapies limits the overall window of their effectiveness to treat patients with LUAD. We sought to determine the extent to which ISRAs could be used not just in *EGFR*-mutated LUAD, but as a general model of acquired resistance to agents targeting the RTK/RAS pathway including the covalent KRAS^{G12C} inhibitors sotorasib (Fig. 4A) and adagrasib (Fig. 4B) in KRAS^{G12C}-mutated (H358, H1373) LUAD cells, the MEK inhibitor trametinib in both *KRAS (non-G12C)*-mutated (H727) and *NF1*-LOF (H1838) LUAD cells (Fig. 4C), the farnesyltransferase inhibitor (FTI) tipifarnib in *HRAS*-mutated LUAD (H1915) and rhabdomyosarcoma (SMS-CTR) cells (Fig. 4D). To establish the doses of each inhibitor that inhibits survival (≥ EC_{50}) in the panel of RAS pathway-mutated cell lines, cells were treated with increasing doses of the indicated inhibitor and cell viability was assesses four days after treatment (Fig. S4); for KRAS^{G12C} and MEK inhibitors dose response curves were performed in 3D culture as *KRAS*-mutated cells show variable responses to either *KRAS* depletion or KRAS^{G12C} inhibition in 2D culture (*39-48*). EC_{50} – EC_{90} values for each drug/cell line combination are shown in Fig. 4E. ISRAs were then performed using inhibitory doses (~EC_{50} – EC_{85}) for each inhibitor/cell line combination. For each cell line, lower doses of the targeted inhibitor corresponding to the EC_{50}-EC_{75} caused a 1–3-week delay in the outgrowth of cells, whereas cells treated with ≥ EC_{80} of inhibitor showed prolonged growth arrest before regaining proliferative capacity (Fig. 4A-D) indicating that these cultures had become resistant to the indicated targeted therapy. These data show that, in addition to

modeling osimertinib, ISRAs can be used to model acquired resistance to multiple therapies targeting the RTK/RAS/ERK pathway.

Discussion

Oncogene-targeted therapies have revolutionized cancer treatment. However, single-agent targeting of mutated oncogenes often shows less than optimal results, as both intrinsic and acquired resistance can limit the overall effectiveness of these agents. Efforts to identify combination therapies have focused on identifying synthetic lethal targets that enhance therapeutic efficacy and overcome intrinsic resistance to oncogene-targeted therapies. Studies that aim to overcome acquired resistance focus on identifying and treating acquired resistance after it occurs. In contrast, studies to assess the extent to which drug combinations can delay the onset of acquired resistance and thereby prolong the initial treatment window are lacking due to the paucity of cell culture methods designed to assess acquired resistance. Here, we describe a novel *in situ* resistance assay, performed in a 96-well culture format, that allows easy assessment of therapeutic resistance and isolation of therapy-resistant populations (Fig. 5).

As a model for assay development, we used osimertinib resistance in *EGFR*-mutated LUAD. Osimertinib is well-established as first-line therapy for patients with *EGFR*-mutated LUAD (*49, 50*), the mechanisms driving acquired resistance are well defined (*23-32*), and mechanism-based treatment of acquired resistance is largely unsuccessful since most patients develop tumors harboring multiple parallel resistance mechanisms simultaneously (*5*). We found that osimertinib resistance could be reliably

modeled in *EGFR*-mutated LUAD cell lines using doses of osimertinib defined by the dose-response curves for individual cell lines dose-response curves. Similar to patient populations, osimertinib-resistant populations isolated from resistance assays showed resistance driven by multiple RTK-dependent mechanisms so that individual RTK inhibitors were insufficient to target these cells. In contrast, pan-RTK inhibition using an inhibitor of the proximal RTK signaling intermediate SHP2 synergistically enhanced the efficacy and potency of osimertinib across osimertinib resistant populations. However, even though SHP2 inhibition synergized with osimertinib to kill resistant populations, combined EGFR/SHP2 inhibition produced only ~70% killing, highlighting the need for combinations that block the development of resistance rather than treating resistant tumors.

A majority of osimertinib resistance is driven by RTK reactivation, thus, pan-RTK inhibition has the potential to circumvent the development of most forms of osimertinib resistance. Indeed, we show that SHP2 inhibition both delayed the onset of osimertinib resistance and limited the overall percentage of populations able to become osimertinib resistant. Downstream of RTKs, the SHP2 phosphatase acts as an adaptor to recruit the RASGEFs SOS1 and SOS2 to receptor complexes and promote RAS activation. In two parallel sets of studies, proximal RTK inhibition, via either *SOS2* deletion (*51*) or SOS1 inhibition (*52*), similarly limited RTK-driven acquired resistance in LUAD. In addition to SHP2 inhibition, *SOS2* KO significantly limited the overall percentage of *EGFR*-mutated LUAD populations able to become osimertinib resistant (*51*). Further analysis of 59 NT and 33 *SOS2* KO osimertinib-resistant populations showed that *SOS2* KO blocked RTK-PI3K dependent osimertinib resistance, and those *SOS2* KO

populations able to become osimertinib resistant did so by histological transformation. The finding that SOS2 was required for RTK-PI3K signaling in osimertinib resistance aligns with previous findings that SOS2 was critical for RTK-PI3K signaling in *KRAS*-mutated LUAD cells (*53, 54*), and highlights the importance of SOS2 as a therapeutic target in LUAD.

In another study, SOS1 inhibition with BI-3406 (*55*) both enhanced the efficacy of and limited the development of acquired resistance to the MEK inhibitor trametinib in $KRAS^{G12}$-mutatated LUAD cells (*52*). The effect of SOS1 inhibition on trametinib resistance was similarly RTK-PI3K pathway dependent, as *PIK3CA* co-mutations ablated the ability of SOS1 inhibition to limit osimertinib resistance. The importance of RTK-PI3K signaling to both osimertinib (*51, 56*) and trametinib (*52*) resistance reinforces the hypothesis that LUADs are RTK/RAS pathway addicted (*57-61*). The findings that pan-RTK inhibition, via blocking SHP2, SOS1, or SOS2, blocks resistance to two distinct RTK/RAS pathway inhibitors in LUAD suggests that inhibiting proximal RTK signaling may be general strategy to limit resistance to RKT/RAS pathway inhibitors in LUAD (*61*).

Finally, our approach to assessing osimertinib resistance *in situ* can be easily adopted to multiple additional RTK/RAS pathway inhibitors with similar objectively defined drug-dosing parameters (Fig. 4 and (*52*)). While studies that identify synergistic drug targets to boost therapeutic efficacy to RTK/RAS pathway inhibitors abound, there has been a paucity of assays to systematically assess the extent to which these same combinations can limit acquired resistance. We propose that *in situ* resistance assays, performed over a 6–12-week period, fill this gap in our arsenal of studies assessing

combination therapies for cancer treatment. The ease of testing multiple combinations simultaneously, combined with the recent decision by the FDA to no longer requires animal testing for approval of new drugs (*62*), make *in situ* resistance assays a cost-effective alternative to long-term animal studies when evaluating therapeutic combinations.

Methods

Cell culture

Cell lines were cultured at 37°C and 5% CO_2. HCC827, NCI-H1975, PC9, PC9-TM, H358, H1373, H727, H1838, and H1915 cells were maintained in Roswell Park Memorial Institute medium (RPMI), SMS-CTR cells were maintained in Dulbecco's Modified Eagles Medium (DMEM), each supplemented with 10% fetal bovine serum and 1% penicillin-streptomycin. Osimertinib-resistant (OR1-7) H1975 cells were isolated from ISRAs treated with 150 or 300 nM osimertinib for > 6 weeks. OR1-7 populations were maintained under osimertinib selection during expansion.

Inhibitor studies

Single dose-response studies: For adherent studies, cells were seeded at 500 cells per well in 100 μL in the inner-60 wells of 96-well white-walled culture plates (Perkin Elmer) and allowed to attach for 24 hours prior to drug treatment. For 3D spheroid studies, cells were seeded at 500-1,000 cells per well in 100 μL in the inner-60 wells of 96-well ultra-low attachment round bottomed plates (Corning #7007) or Nunc Nucleon Sphera microplates (ThermoFisher # 174929) and allowed to coalesce as spheroids for 24-48 hours prior to drug treatment. Cells were treated with drug for 96 hours prior to assessment of cell viability using CellTiter-Glo® 2.0. Data were analyzed by non-linear regression using Prism 9.

Assessment of synergy: Cells were seeded at 200 cells per well in 40 μL in the inner-312 wells of 384-well white-walled culture plates (Perkin Elmer) and allowed to attach for 24-hours prior to drug treatment. To assess the effectiveness of secondary therapies

+/- osimertinib, cells were treated with increasing doses of crizotinib, cabozantinib, infigratinib, selpercatinib, linsitinib, SGI-7079, dasatinib, or RMC-4550 +/- 10 nM osimertinib. To assess the extent to which each secondary inhibitor enhanced the effectiveness of osimertinib, cells were treated with increasing doses of osimertinib +/- 100 nM or 300 nM of one of the above inhibitors. To assess drug-drug synergy across a matrix of dose combinations for the osimertinib/RMC-4550 combination, cells were treated with increasing doses of RMC-4550 alone, osimertinib alone, or osimertinib + RMC-4550 in a 6x10 matrix of drug combinations on a semilog scale. Cells were treated with drug for 96 hours prior to assessment of cell viability using CellTiter-Glo® 2.0. Values were normalized to DMSO controls and assessment of synergy via Bliss Independence analysis was completed as reported previously (*63*). To deconvolute synergistic synergy versus potency, data were analyzed by Multi-dimensional Synergy of Combinations (MuSyC) Analysis (*37, 38*) using an online tool (https://musyc.lolab.xyz) and are presented as mean +/- 95% confidence interval.

In situ resistance assays (ISRAs)

Cells were seeded at 250 cells/well in 100 μL in replicate 96-well tissue culture plates and allowed to adhere for 24 hours prior to drug treatment. Plates were then either fed with an additional 100 μL of media or treated with the indicated single dose of targeted inhibitor (osimertinib, sotorasib, adagrasib, trametinib, or tipifarnib) corresponding to approximately the EC_{50} – EC_{85} dose of that drug. For Fig. 3, plates were treated with the indicated drug combinations. The inner 60 wells of each plate were assessed weekly for signs of cell growth using a 4 x objective, with wells reaching >50%

confluence scored as resistant. Plates were fed weekly; media was removed from the entire plate in a cell culture hood by quickly inverting the plate into an autoclave bin lined with paper towels to avoid cross-contamination of wells and plates were fed with a multi-channel repeating pipettor. Data are plotted as a Kaplan-Meyer survival curve; significance was assessed by comparing Kaplan-Meyer curves using Prism 9.

Phospho-tyrosine Array Analysis

Cells were lysed in RIPA buffer (1% NP-40, 0.1% SDS, 0.1% Na-deoxycholate, 10% glycerol, 0.137 M NaCl, 20 mM Tris pH [8.0], protease (Biotool #B14002) and phosphatase (Biotool #B15002) inhibitor cocktails) for 20 minutes at 4°C and spun at 10,000 RPM for 10 minutes. Clarified lysates were diluted to 1 mg/mL in RIPA buffer prior to assessing for RTK phosphorylation using a Human RTK Phosphorylation Array G1 (RayBiotech, AAH-PRTK-G1-8) per manufacturer's instructions. Slides were shipped to RayBiotech for data acquisition. For each phosphorylated protein, data were normalized to the average level of phosphorylation observed from two independent isolates of H1975 parental lysate.

Acknowledgments

This work was supported by funding from the NIH (R01 CA255232 and R21 CA267515 to R.L.K.) and the CDMRP Lung Cancer Research Program (LC180213 to R.L.K.). The funders had no role in the study design, data collection and interpretation, or the decision to submit the work for publication. The opinions and assertions expressed herein are those of the authors and are not to be construed as reflecting the views of Uniformed Services University of the Health Sciences or the United States Department of Defense. Materials are available upon request from R.L.K.

Author Contributions

NES, PLT, and RLK designed the experiments and analyzed the data; NES, PLT and RLK performed most of the experiments; AJL and BRD performed resistance assays; JEH assisted with dose response curves. NES and RLK wrote the manuscript, BRD edited the manuscript.

Competing Interests

The authors declare no competing financial interests.

Fig. 1

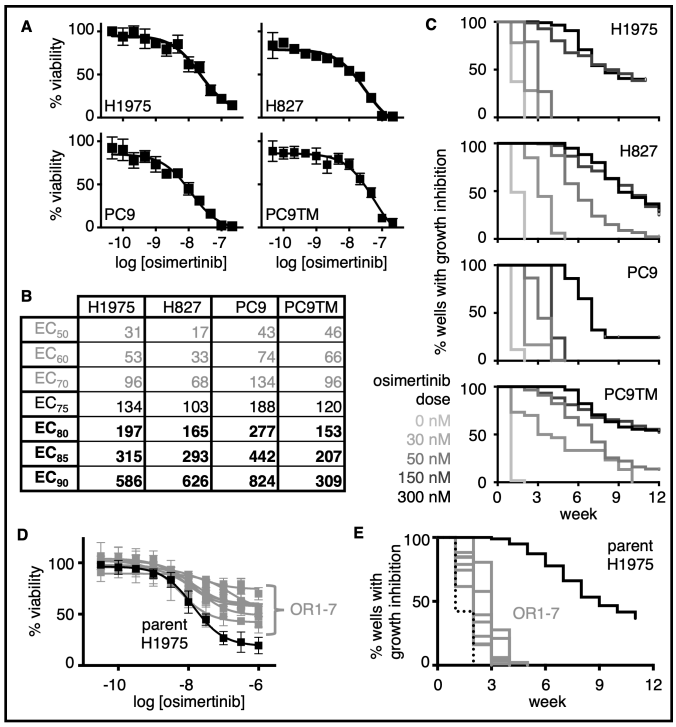

	H1975	H827	PC9	PC9TM
EC_{50}	31	17	43	46
EC_{60}	53	33	74	66
EC_{70}	96	68	134	96
EC_{75}	134	103	188	120
EC_{80}	**197**	**165**	**277**	**153**
EC_{85}	**315**	**293**	**442**	**207**
EC_{90}	**586**	**626**	**824**	**309**

Fig 1. Modeling osimertinib resistance in situ.
(**A** to **B**) Dose response curves (A) and EC_{50} – EC_{90} values (B) for the indicated *EGFR*-mutated LUAD cell lines treated with osimertinib under anchorage-dependent conditions. (**C**) *In situ* resistance assays for the indicated EGFR-mutated LUAD cells treated with the indicated dose of osimertinib. (**D** to **E**) Dose response curves (D) and in situ resistance assays (E) assessing osimertinib sensitivity in parental H1975 cells (black) and osimertinib-resistant H1975 populations OR1-OR7 (grey) isolated from cells treated with 150-300 nM osimertinib for ≥ six weeks. Curves comparing individual osimertinib-resistant populations to parental H1975 cells are shown in Fig. S1.

Fig. 2.

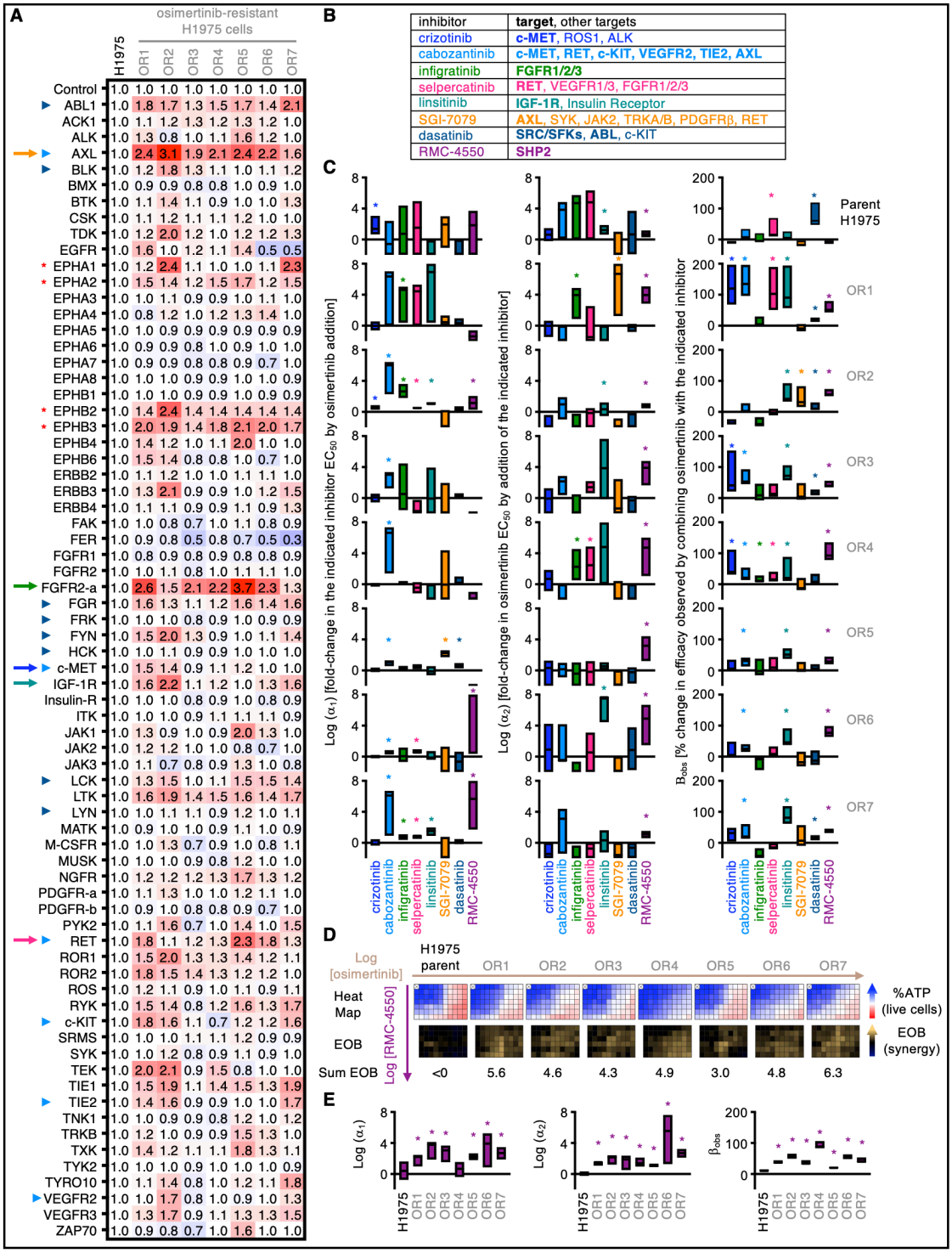

Fig 2. Isolated osimertinib resistant clones show activated RTKs and are sensitive to SHP2 inhibition.

(**A**) Relative change in RTK phosphorylation in OR1-7 H1975 populations normalized to parental H1975 controls from RTK phosphorylation arrays in Fig. S2. Red numbers indicate increased tyrosine phosphorylation of the indicated kinase over parental controls, blue numbers indicate decreased tyrosine phosphorylation. Colored arrows indicate drug targets for inhibitors (B) tested in combination with osimertinib in (C), large arrows indicate the primary drug target whereas small arrows indicate the multiple targets for a given color coded inhibitor. * Indicates EPH receptor family members with increased phosphorylation across resistant clones. (**B**) Inhibitors to common osimertinib resistance mechanisms observed in A; bold indicated the primary drug target for each inhibitor. (**C**) Synergy scores showing the relative abilities of osimertinib to enhance the efficacy of secondary inhbitors [Log(α_1)] or these inhibitors enhance the efficacy [Log(α_2)] or observed potency (β_{obs}) of osimertinib in OR1-7 H1975 populations. (**D**) Heat maps of cell viability (top) and excess over Bliss (EOB, bottom) for OR1-7 H1975 populations treated with increasing (semilog) doses of RMC-4550 (10^{-8} – $10^{-5.5}$), osimertinib ($10^{-10.5}$ – 10^{-6}), or the combination of RMC-4550 + osimertinib over a 6×10 dose matrix. Sum EOB indicates the extent of synergy across the dose matrix. (**E**) Synergy scores showing the relative changes in efficacy or observed potency of in parental or OR1-7 H1975 populations treated with osimertinib + RMC-4550 from (D).

Fig. 3

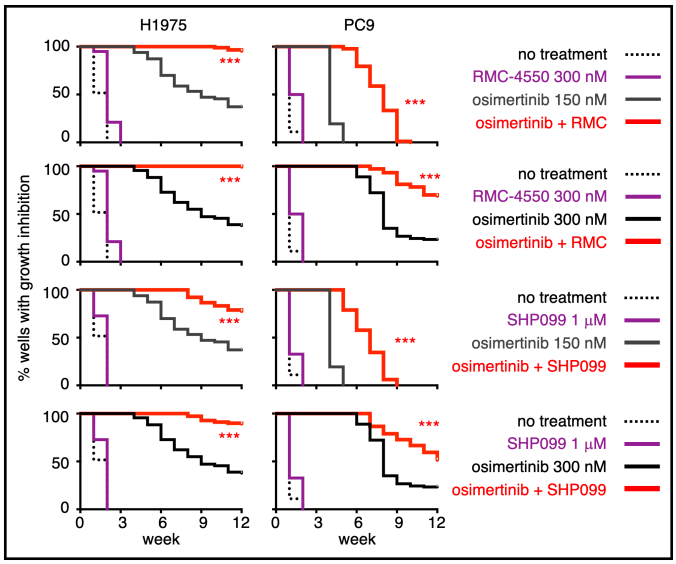

Fig 3. **SHP2 inhibition limits the development of osimertinib resistance.**

In situ resistance assays for *EGFR*-mutated H1975 and PC9 cells left untreated (black, dashed) treated with osimertinib alone at 150 (dark grey) or 300 nM (black), treated with a SHP2 inhibitor alone (RMC-4550 at 300 nM or SHP099 at 1 mM) (purple), or treated with the combination of osimertinib + a SHP2 inhibitor (RMC-4550 or SHP099, red). Data are plotted as a Kaplan-Meyer survival curve. *** $p<0.001$ vs single drug treatment.

Fig. 4

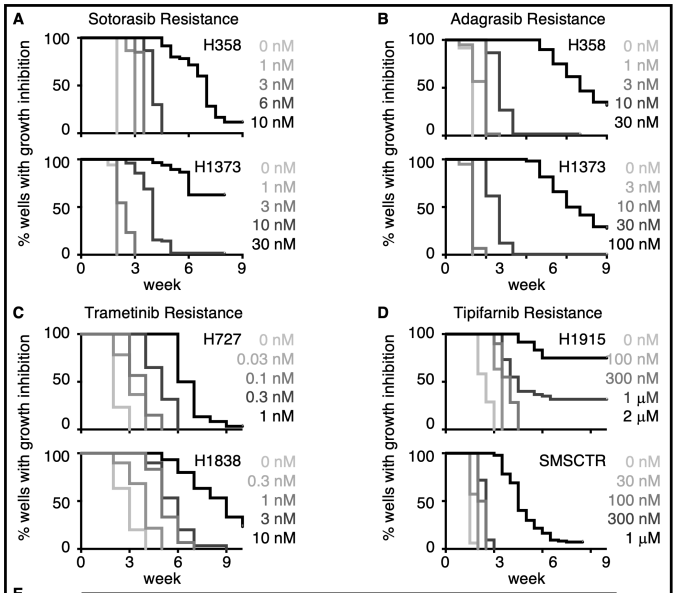

E

	Sotorasib (3D)		Adagrasib (3D)		Trametinib (3D)		Tipifarnib (2D)	
	H358	H1373	H358	H1373	H727	H1838	H1915	SMS
EC_{50}	4	12	8	25	0.2	0.5	45	108
EC_{60}	5	16	12	33	0.3	1	85	161
EC_{70}	7	21	18	45	0.4	3	169	250
EC_{75}	8	25	23	54	0.6	5	249	321
EC_{80}	**10**	**31**	**31**	**66**	**0.8**	**9**	**388**	**428**
EC_{85}	**12**	**39**	**44**	**85**	**1.1**	**20**	**666**	**605**
EC_{90}	**16**	**53**	**70**	**118**	**1.8**	**51**	**1362**	**959**

Fig 4. *In situ* resistance assays can be used to model acquired resistance to RTK/RAS pathway targeted therapies.

(**A** to **D**) *In situ* resistance assays for *KRAS*^{G12C}-mutated H358 and H1373 cells (A, B), *KRAS*^{G12V}-mutated H727 and *NF1*-LOF H1838 cells (C), or *HRAS*-mutated H1915 and SMSCTR cells left untreated or treated with the indicated dose of sotorasib (A), adagrasib (B), trametinib (C), or tipifarnib (D). Data are plotted as a Kaplan-Meyer survival curve. Plates treated with ≥ the EC_{80} dose of a given targeted inhibitor (see bold values in E) showed an extended inhibition of growth followed by outgrowth of individual colonies consistent with true drug resistance. (**E**) EC_{50} – EC_{90} values from dose response curves assessing sotorasib (H358, H1373), adagrasib (H358, H1373), trametinib (H727, H1838), or tipifarnib (H1915, SMSCTR) sensitivity.

Fig. 5

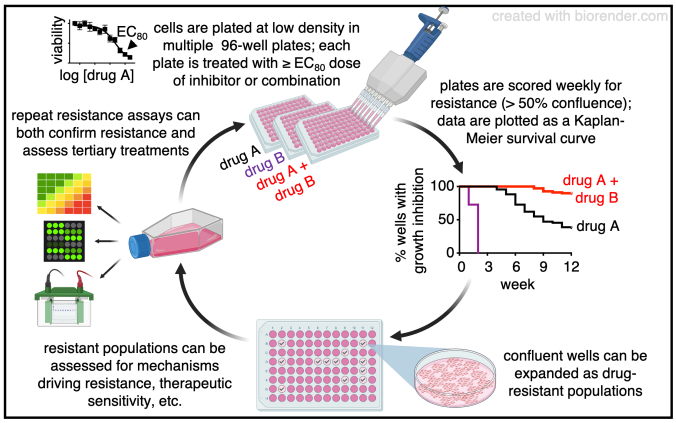

Fig. 5. Framework for assessing acquired resistance *in situ*.

References

1. C. Gridelli *et al.*, Non-small-cell lung cancer. *Nat Rev Dis Primers* **1**, 15009 (2015).
2. D. Plana, A. C. Palmer, P. K. Sorger, Independent Drug Action in Combination Therapy: Implications for Precision Oncology. *Cancer Discov* **12**, 606-624 (2022).
3. J. R. Pritchard, D. A. Lauffenburger, M. T. Hemann, Understanding resistance to combination chemotherapy. *Drug Resist Updat* **15**, 249-257 (2012).
4. I. Bozic *et al.*, Evolutionary dynamics of cancer in response to targeted combination therapy. *Elife* **2**, e00747 (2013).
5. N. Roper *et al.*, Clonal Evolution and Heterogeneity of Osimertinib Acquired Resistance Mechanisms in EGFR Mutant Lung Cancer. *Cell Rep Med* **1**, (2020).
6. N. Tanaka *et al.*, Clinical Acquired Resistance to KRAS(G12C) Inhibition through a Novel KRAS Switch-II Pocket Mutation and Polyclonal Alterations Converging on RAS-MAPK Reactivation. *Cancer Discov* **11**, 1913-1922 (2021).
7. K. Fu, F. Xie, F. Wang, L. Fu, Therapeutic strategies for EGFR-mutated non-small cell lung cancer patients with osimertinib resistance. *J Hematol Oncol* **15**, 173 (2022).
8. G. R. Oxnard *et al.*, Assessment of Resistance Mechanisms and Clinical Implications in Patients With EGFR T790M-Positive Lung Cancer and Acquired Resistance to Osimertinib. *JAMA Oncol* **4**, 1527-1534 (2018).
9. R. Bernards, Finding effective cancer therapies through loss of function genetic screens. *Curr Opin Genet Dev* **24**, 23-29 (2014).
10. O. Shalem *et al.*, Genome-scale CRISPR-Cas9 knockout screening in human cells. *Science* **343**, 84-87 (2014).
11. G. R. Anderson *et al.*, A Landscape of Therapeutic Cooperativity in KRAS Mutant Cancers Reveals Principles for Controlling Tumor Evolution. *Cell Rep* **20**, 999-1015 (2017).
12. S. Ohara, K. Suda, T. Mitsudomi, Cell Line Models for Acquired Resistance to First-Line Osimertinib in Lung Cancers-Applications and Limitations. *Cells* **10**, (2021).
13. Z. H. Tang *et al.*, Increased Expression of IRE1alpha Associates with the Resistant Mechanism of Osimertinib (AZD9291)-resistant non-small Cell Lung Cancer HCC827/OSIR Cells. *Anticancer Agents Med Chem* **18**, 550-555 (2018).
14. Z. H. Tang *et al.*, Characterization of osimertinib (AZD9291)-resistant non-small cell lung cancer NCI-H1975/OSIR cell line. *Oncotarget* **7**, 81598-81610 (2016).
15. J. Codony-Servat *et al.*, Hsp90 inhibitors enhance the antitumoral effect of osimertinib in parental and osimertinib-resistant non-small cell lung cancer cell lines. *Transl Lung Cancer Res* **8**, 340-351 (2019).
16. K. Fukuda *et al.*, Glycogen synthase kinase-3 inhibition overcomes epithelial-mesenchymal transition-associated resistance to osimertinib in EGFR-mutant lung cancer. *Cancer Sci* **111**, 2374-2384 (2020).
17. Y. Murakami *et al.*, AXL/CDCP1/SRC axis confers acquired resistance to osimertinib in lung cancer. *Sci Rep* **12**, 8983 (2022).
18. J. M. Fernandes Neto *et al.*, Multiple low dose therapy as an effective strategy to treat EGFR inhibitor-resistant NSCLC tumours. *Nat Commun* **11**, 3157 (2020).

19. K. J. Frank *et al.*, Extensive preclinical validation of combined RMC-4550 and LY3214996 supports clinical investigation for KRAS mutant pancreatic cancer. *Cell Rep Med* **3**, 100815 (2022).
20. K. J. Kurppa *et al.*, Treatment-Induced Tumor Dormancy through YAP-Mediated Transcriptional Reprogramming of the Apoptotic Pathway. *Cancer Cell* **37**, 104-122.e112 (2020).
21. E. M. Tricker *et al.*, Combined EGFR/MEK Inhibition Prevents the Emergence of Resistance in EGFR-Mutant Lung Cancer. *Cancer Discov* **5**, 960-971 (2015).
22. R. J. Nichols *et al.*, RAS nucleotide cycling underlies the SHP2 phosphatase dependence of mutant BRAF-, NF1- and RAS-driven cancers. *Nat Cell Biol* **20**, 1064-1073 (2018).
23. C. A. Eberlein *et al.*, Acquired Resistance to the Mutant-Selective EGFR Inhibitor AZD9291 Is Associated with Increased Dependence on RAS Signaling in Preclinical Models. *Cancer Res* **75**, 2489-2500 (2015).
24. P. Shi *et al.*, Met gene amplification and protein hyperactivation is a mechanism of resistance to both first and third generation EGFR inhibitors in lung cancer treatment. *Cancer Lett* **380**, 494-504 (2016).
25. S. La Monica *et al.*, Trastuzumab emtansine delays and overcomes resistance to the third-generation EGFR-TKI osimertinib in NSCLC EGFR mutated cell lines. *J Exp Clin Cancer Res* **36**, 174 (2017).
26. M. Mancini *et al.*, An oligoclonal antibody durably overcomes resistance of lung cancer to third-generation EGFR inhibitors. *EMBO Mol Med* **10**, 294-308 (2018).
27. D. Romaniello *et al.*, A Combination of Approved Antibodies Overcomes Resistance of Lung Cancer to Osimertinib by Blocking Bypass Pathways. *Clin Cancer Res* **24**, 5610-5621 (2018).
28. J. H. Park *et al.*, Activation of the IGF1R pathway potentially mediates acquired resistance to mutant-selective 3rd-generation EGF receptor tyrosine kinase inhibitors in advanced non-small cell lung cancer. *Oncotarget* **7**, 22005-22015 (2016).
29. D. Kim *et al.*, AXL degradation in combination with EGFR-TKI can delay and overcome acquired resistance in human non-small cell lung cancer cells. *Cell Death Dis* **10**, 361 (2019).
30. H. Taniguchi *et al.*, AXL confers intrinsic resistance to osimertinib and advances the emergence of tolerant cells. *Nat Commun* **10**, 259 (2019).
31. K. Namba *et al.*, Activation of AXL as a Preclinical Acquired Resistance Mechanism Against Osimertinib Treatment in EGFR-Mutant Non-Small Cell Lung Cancer Cells. *Mol Cancer Res* **17**, 499-507 (2019).
32. T. Jimbo *et al.*, DS-1205b, a novel selective inhibitor of AXL kinase, blocks resistance to EGFR-tyrosine kinase inhibitors in a non-small cell lung cancer xenograft model. *Oncotarget* **10**, 5152-5167 (2019).
33. S. Raoof *et al.*, Targeting FGFR overcomes EMT-mediated resistance in EGFR mutant non-small cell lung cancer. *Oncogene* **38**, 6399-6413 (2019).
34. M. G. Terp *et al.*, Combined FGFR and Akt pathway inhibition abrogates growth of FGFR1 overexpressing EGFR-TKI-resistant NSCLC cells. *NPJ Precis Oncol* **5**, 65 (2021).
35. R. Wang *et al.*, Transient IGF-1R inhibition combined with osimertinib eradicates AXL-low expressing EGFR mutated lung cancer. *Nat Commun* **11**, 4607 (2020).

36. Z. Piotrowska *et al.*, Landscape of Acquired Resistance to Osimertinib in EGFR-Mutant NSCLC and Clinical Validation of Combined EGFR and RET Inhibition with Osimertinib and BLU-667 for Acquired RET Fusion. *Cancer Discov* **8**, 1529-1539 (2018).
37. C. T. Meyer *et al.*, Quantifying Drug Combination Synergy along Potency and Efficacy Axes. *Cell Syst* **8**, 97-108 e116 (2019).
38. D. J. Wooten, C. T. Meyer, A. L. R. Lubbock, V. Quaranta, C. F. Lopez, MuSyC is a consensus framework that unifies multi-drug synergy metrics for combinatorial drug discovery. *Nature Communications* **12**, 4607 (2021).
39. C. Scholl *et al.*, Synthetic lethal interaction between oncogenic KRAS dependency and STK33 suppression in human cancer cells. *Cell* **137**, 821-834 (2009).
40. A. Singh *et al.*, A gene expression signature associated with "K-Ras addiction" reveals regulators of EMT and tumor cell survival. *Cancer Cell* **15**, 489-500 (2009).
41. A. Singh *et al.*, TAK1 inhibition promotes apoptosis in KRAS-dependent colon cancers. *Cell* **148**, 639-650 (2012).
42. O. A. Balbin *et al.*, Reconstructing targetable pathways in lung cancer by integrating diverse omics data. *Nat Commun* **4**, 2617 (2013).
43. S. Lamba *et al.*, RAF suppression synergizes with MEK inhibition in KRAS mutant cancer cells. *Cell Rep* **8**, 1475-1483 (2014).
44. Z. Zhang, G. Jiang, F. Yang, J. Wang, Knockdown of mutant K-ras expression by adenovirus-mediated siRNA inhibits the in vitro and in vivo growth of lung cancer cells. *Cancer Biol Ther* **5**, 1481-1486 (2006).
45. S. Fujita-Sato *et al.*, Enhanced MET Translation and Signaling Sustains K-Ras-Driven Proliferation under Anchorage-Independent Growth Conditions. *Cancer Res* **75**, 2851-2862 (2015).
46. F. McCormick, KRAS as a Therapeutic Target. *Clin Cancer Res* **21**, 1797-1801 (2015).
47. A. Rotem *et al.*, Alternative to the soft-agar assay that permits high-throughput drug and genetic screens for cellular transformation. *Proc Natl Acad Sci U S A* **112**, 5708-5713 (2015).
48. M. R. Janes *et al.*, Targeting KRAS Mutant Cancers with a Covalent G12C-Specific Inhibitor. *Cell* **172**, 578-589 e517 (2018).
49. S. S. Ramalingam *et al.*, Overall Survival with Osimertinib in Untreated, EGFR-Mutated Advanced NSCLC. *N Engl J Med* **382**, 41-50 (2020).
50. J. C. Soria *et al.*, Osimertinib in Untreated EGFR-Mutated Advanced Non-Small-Cell Lung Cancer. *N Engl J Med* **378**, 113-125 (2018).
51. P. L. Theard *et al.*, SOS2 regulates the threshold of mutant EGFR-dependent oncogenesis. *bioRxiv*, 2023.2001.2020.524989 (2023).
52. B. D. Daley *et al.*, SOS1 and KSR1 modulate MEK inhibitor responsiveness to target resistant cell populations based on PI3K and KRAS mutation status. *bioRxiv*, 2022.2012.2006.519395 (2023).
53. E. Sheffels *et al.*, Oncogenic RAS isoforms show a hierarchical requirement for the guanine nucleotide exchange factor SOS2 to mediate cell transformation. *Sci Signal* **11**, (2018).

54. E. Sheffels, N. E. Sealover, P. L. Theard, R. L. Kortum, Anchorage-independent growth conditions reveal a differential SOS2 dependence for transformation and survival in RAS-mutant cancer cells. *Small GTPases* **12**, 67-78 (2021).
55. M. H. Hofmann *et al.*, BI-3406, a Potent and Selective SOS1-KRAS Interaction Inhibitor, Is Effective in KRAS-Driven Cancers through Combined MEK Inhibition. *Cancer Discov* **11**, 142-157 (2021).
56. K. Jacobsen *et al.*, Convergent Akt activation drives acquired EGFR inhibitor resistance in lung cancer. *Nat Commun* **8**, 410 (2017).
57. J. Rotow, T. G. Bivona, Understanding and targeting resistance mechanisms in NSCLC. *Nat Rev Cancer* **17**, 637-658 (2017).
58. R. C. Doebele, Acquired Resistance Is Oncogene and Drug Agnostic. *Cancer Cell* **36**, 347-349 (2019).
59. A. Vaishnavi *et al.*, EGFR Mediates Responses to Small-Molecule Drugs Targeting Oncogenic Fusion Kinases. *Cancer Res* **77**, 3551-3563 (2017).
60. M. G. Ferrara *et al.*, Oncogene-Addicted Non-Small-Cell Lung Cancer: Treatment Opportunities and Future Perspectives. *Cancers (Basel)* **12**, (2020).
61. E. Sheffels, R. L. Kortum, Breaking Oncogene Addiction: Getting RTK/RAS-Mutated Cancers off the SOS. *J Med Chem* **64**, 6566-6568 (2021).
62. M. Wadman, FDA no longer has to require animal testing for new drugs. *Science* **379**, 127-128 (2023).
63. P. L. Theard *et al.*, Marked synergy by vertical inhibition of EGFR signaling in NSCLC spheroids shows SOS1 is a therapeutic target in EGFR-mutated cancer. *Elife* **9**, (2020).